tgp v1.1: an R package for Bayesian semiparametric and nonstationary regression by treed Gaussian process models

Robert B. Gramacy
Department of Applied Math & Statistics
University of California, Santa Cruz
rbgramacy@ams.ucsc.edu

February 24, 2006

The tgp package for R [18] is a tool for fully Bayesian, nonparametric, semiparametric, and nonstationary regression by treed Gaussian processes with jumps to the limiting linear model. Special cases also implemented include Bayesian linear models, linear CART, stationary separable and isotropic Gaussian processes. In addition to inference and posterior prediction 1-d and 2-d plotting with higher dimension projection and slice capabilities and tree drawing functions (requiring maptree and combinat libraries) are also provided for visualization of tgp-class output.

This document is intended to familiarize a (potential) user of tgp with the models and analyzes available in the package. After a brief overview, the brunt of this document consists of examples on mainly synthetic and randomly generated data which illustrate the various functions and methodologies implemented by the package. This document has been authored in Sweave (try help(Sweave)). This means that (1) the code quoted throughout is certified by R, and the Stangle command can be used to extract it; and (2) that this is a dynamic document, i.e., each time the document is compiled the figures and analyzes are re-run and updated based on random data and initialization [I suggest you try this nifty feature].

The outline of this tutorial is as follows. Section 1 introduces the functions and associated regression models implemented by the tgp package, including plotting and visualization methods. The Bayesian mathematical specification of these models is contained in Section 2. In Section 3 the functions and methods implemented in the package are illustrated by example. The appendix covers miscellaneous topics such as how to link with the ATLAS libraries for fast linear algebra routines, and some of the details of implementation.

This document is intended as a tutorial, or initial guide, to the tgp package covering key points, concepts, and methods. It was not meant to serve as an instruction manual. For more detailed documentation of the functions

R function	Ingredients	Description
blm	LLM	Linear Model
btlm	T	Linear CART
bgp	GP	GP Regression
bgpllm	GP, LLM	GP with jumps to the LLM
btgp	T, GP	treed GP Regression
btgpllm	T, GP, LLM	treed GP with jumps to the LLM
tgp		Master interface for the above methods

Table 1: Bayesian regression models implemented by the `tgp` package

contained in the package, see the package help-manuals. At an `R` prompt, type `help(package=tgp)`. PDF documentation is also available on the world-wide-web.

`http://www.cran.r-project.org/doc/packages/tgp.pdf`

1 What is implemented?

The `tgp` package contains implementations of six Bayesian multivariate regression models and functions for visualizing posterior predictive surfaces. These models, and the functions which implement them, are outlined in Section 1.1. Details pertaining to the mathematics of model specification, including prior and posterior distributions, is deferred to Section 2. Also implemented in the package are functions which aid in the sequential design of experiments for `tgp`-class models, which is what I call *adaptive sampling*. These functions are introduced at the end of this section.

1.1 Bayesian regression models

The six regression models implemented in package are summarized in Table 1. They include combinations of treed partition models, (limiting) linear models, and Gaussian process models as indicated by T, LLM, & GP in the center column of the table. The details of model specification and inference are contained in Section 2. Each is a fully Bayesian regression model, and in the table they are ordered by some notion of "flexibility". These `b*` functions, as I call them, are wrappers around the master `tgp` function which is an interface to `C` code implementing Bayesian treed Gaussian process models, with jumps to the limiting linear model (LLM). Each `b*` function implements a special case of the treed GP (`tgp`) model.

It is possible to invoke any of the `b*` methods directly via first calling the the `tgp.default.params` function and then the `tgp` function after some minor adjustments to the default parameterization. The help file for `tgp` shows how to do this for many of the examples in this document. The `b*` functions are intended as the main interface to the Bayesian multivariate regression models,

so little further attention to the tgp master function will be included here. That is, with the exception of one example in Section 3.4 where a more custom model is needed in order to capture input dependent noise, and a remark here that the easiest way to see how the master tgp function implements one of the b* methods is to simply type the name of the function of interest into R. For example, to see the implementation of bgp, type:

```
> bgp
```

```
function (X, Z, XX = NULL, bprior = "bflat", corr = "expsep",
    BTE = c(1000, 4000, 2), R = 1, m0r1 = FALSE, pred.n = TRUE,
    ds2x = FALSE, ego = FALSE)
{
    n <- dim(X)[1]
    if (is.null(n)) {
        n <- length(X)
        X <- matrix(X, nrow = n)
        d <- 1
    }
    else {
        d <- dim(X)[2]
    }
    params <- tgp.default.params(d + 1)
    params$bprior <- bprior
    params$corr <- corr
    params$tree <- c(0, 0, 10)
    params$gamma <- c(0, 0.2, 0.7)
    return(tgp(X, Z, XX, BTE, R, m0r1, FALSE, params, pred.n,
        ds2x, ego))
}
```

The output (return-value) of tgp and the b* functions is a list-object of class "tgp". This is what is meant by a "tgp-class" object. This object retains all of the relevant information necessary to summarize posterior predictive inference, maximum *a' posteriori* (MAP) trees, and statistics for adaptive sampling. Information about its actual contents is contained in the help files for the tgp and b* functions. Generic print and plot methods are defined for tgp-class objects. The plot function is discussed below. The print function simply provides a list of the names of the fields comprising a tgp-class object.

1.1.1 Plotting and visualization

The two main functions provided by the tgp package for visualization are plot.tgp, inheriting from the generic plot method, and a function called tgp.trees for graphical visualization of MAP trees.

The plot.tgp function can make plots in 1-d or 2-d. Of course, if the data are 1-d, the plot is in 1-d. If the data are 2-d, or higher, they are 2-d image

or perspective plots unless a 1-d projection argument is supplied. Data which is 3-d, or higher, requires projection down to 2-d or 1-d, or specification of a 2-d slice. The `plot.tgp` default is to make a projection onto the first two input variables. Alternate projections are specified as an argument (`proj`) to the function. Likewise, there is also an argument (`slice`) which allows one to specify which slice of the posterior predictive data is desired. For models that use treed partitioning (those with a T in the center column of Table 1), the `plot.tgp` function will overlay the region boundaries of the MAP tree ($\hat{T}$) found during MCMC.

A few notes on 2-d plotting of `tgp`-class objects:

- 2-d plotting requires interpolation of the data onto a uniform grid. This is supported by the `tgp` package in two ways: (1) `loess` smoothing, and (2) the `akima` package, available from CRAN. The default is `loess` because it is more stable and does not require installing any further packages. When `akima` works it makes (in my opinion) smarter interpolations. However there are two bugs in the `akima` package, one malign and the other benign, which preclude it from the default position in `tgp`. The malign bug can cause a segmentation fault, and bring down the entire R session. The benign bug produces `NA`'s when plotting data from a grid. For beautiful 2-d plots of gridded data I suggest exporting the `tgp` predictive output to a text file and using `gnuplot`'s 2-d plotting features.

- The current version of this package contains no examples—nor does this document—which demonstrate plotting of data with dimension larger than two. The example provided in Section 3.5 uses 10-d data, however no plotting is required. My thesis [10] contains a detailed analysis of some proprietary 3-d data sampled using a NASA supercomputer.

- The `plot.tgp` function has many more options than are illustrated [in Section 3] of this document. Please refer to the help files for more details.

The `tgp.trees` function provides a graphical representation of the MAP trees of each height encountered by the Markov chain during sampling. The function will not plot trees of height one, i.e., trees with no branching or partitioning. Plotting of trees requires the `maptree` package, which in turn requires the `combinat` package, both available from CRAN.

1.1.2 Speed

This is as good a place as any to make a disclaimer on the computational burdens of some of the modeling functions in this package. Fully Bayesian analyses with MCMC are not the super-speediest of all statistical models. Nor is inference for GP models, classical or Bayesian.

Great care has been taken to make the implementation of Bayesian inference of GP models as efficient as possible [see Appendix B]. However, inference for non-treed GPs for non-linear data can be computationally intense. Two things

are implemented by the package which can help speed things up a bit. The first is direct support for `ATLAS` [23] for fast linear algebra. Details on linking this package with `ATLAS` is contained in Appendix A. The second is an argument called `linburn` to the tree class (T) functions in Table 1. When `linburn = TRUE`, the Markov chain is initialized with a run of the Bayesian linear CART algorithm [4] before burn-in in order to pre-partition the input space using linear models.

1.2 Sequential design of experiments

Sequential design of experiments, a.k.a. *adaptive sampling*, is not implemented by any *single* function in the `tgp` package. Nevertheless, options and functions are provided in order to facilitate the automation of adaptive sampling with `tgp`-class models. A detailed example is included in Section 3.6.

Arguments to `b*` functions, and `tgp`, which aid in adaptive sampling include `ds2x` and `ego`. Both are booleans, i.e., should be set to `TRUE` or `FALSE` (the default for both is `FALSE`). `TRUE` booleans cause the `tgp`-class output list to contain vectors of the similar names which contain statistics that can be used toward adaptive sampling. When `ds2x = TRUE` then the $\Delta\sigma^2(\tilde{\mathbf{x}})$ statistic is computed at each $\tilde{\mathbf{x}} \in$ `XX`, in accordance the ALC (Active Learning–Cohn) algorithm [5]. Likewise, when `ego = TRUE`, statistics for Expected Global Optimization (EGO) [14] are computed in order to asses the expected information gain for each $\tilde{\mathbf{x}} \in$ `XX` about the global minimum. The ALM (Active Learning–Mackay) algorithm [15] is implemented by default in terms of difference in predictive quantiles for the inputs `XX`, which can be accessed via the `ZZ.q` output field. Details and references on the ALM, ALC, and EGO algorithms are provided in Section 2.

Calculation of EGO statistics is considered to be "alpha" functionality in this version of the `tgp` package. It has not been adequately tested, and its implementation is likely to change substantially in future versions of the package.

The functions included in the package which explicitly aid in the sequential design of experiments are `tgp.design` and `dopt.gp`. They are both intended to produce sequential D-optimal candidate designs `XX` at which one or more of the adaptive sampling methods (ALM, ALC, EGO) can gather statistics. The `dopt.gp` function generates D-optimal candidates for a stationary Gaussian process. The `tgp.design` function extracts the MAP tree from a `tgp`-class object and uses `dopt.gp` on each region of the MAP partition in order to get treed sequential D-optimal candidates.

2 Methods and Models

This section provides a quick overview of the statistical models and methods implemented by the `tgp` package. Stationary Gaussian processes (GPs), GPs with jumps to the limiting linear model (LLM; a.k.a. GP LLM), treed partitioning for nonstationary models, and sequential design of experiments (a.k.a. *adaptive*

sampling) concepts for these models are all briefly discussed. Appropriate references are provided for the details. Of course, the best reference is probably my thesis [10].

As a first pass on this document, it might make sense to skip this section and go straight on to the examples in Section 3.

2.1 Stationary Gaussian processes

Below is a hierarchical generative model for a stationary GP with linear tend for data $D = \{\mathbf{X}, \mathbf{Z}\}$.

$$\begin{aligned} \mathbf{Z}|\beta, \sigma^2, \mathbf{K} &\sim N_n(\mathbf{F}\beta, \sigma^2\mathbf{K}) \\ \beta|\sigma^2, \tau^2, \mathbf{W}, \beta_0 &\sim N_{m_X}(\beta_0, \sigma^2\tau^2\mathbf{W}) \\ \beta_0 &\sim N_{m_X}(\boldsymbol{\mu}, \mathbf{B}) \\ \sigma^2 &\sim IG(\alpha_\sigma/2, q_\sigma/2) \\ \tau^2 &\sim IG(\alpha_\tau/2, q_\tau/2) \\ \mathbf{W}^{-1} &\sim W((\rho\mathbf{V})^{-1}, \rho), \end{aligned} \tag{1}$$

where $\mathbf{F} = (\mathbf{1}, \mathbf{X})$, and $\mathbf{W}$ is a $(m_X + 1) \times (m_X + 1)$ matrix. N, IG, and W are the (Multivariate) Normal, Inverse-Gamma, and Wishart distributions, respectively. Constants $\boldsymbol{\mu}, \mathbf{B}, \mathbf{V}, \rho, \alpha_\sigma, q_\sigma, \alpha_\tau, q_\tau$. are treated as known.

The GP correlation structure $\mathbf{K}$ is chosen either from the isotropic power family, or separable power family, with a fixed power p_0 (see below), but unknown (random) range and nugget parameters. Correlation functions used in the `tgp` package take the form $K(\mathbf{x}_j, \mathbf{x}_k) = K^*(\mathbf{x}_j, \mathbf{x}_k) + g\delta_{j,k}$, where $\delta_{\cdot,\cdot}$ is the Kronecker delta function, and K^* is a *true* correlation representative from a parametric family.

All parameters in (1) can be sampled using Gibbs steps, except for the covariance structure and nugget parameters, and their hyperparameters, which can be sampled via Metropolis-Hastings [11, 10].

2.1.1 The nugget

The g term in the correlation function $K(\cdot, \cdot)$ is referred to as the *nugget* in the geostatistics literature [16, 6] and sometimes as *jitter* in the Machine Learning literature [17]. It must always be positive ($g > 0$), and serves two purposes. Primarily, it provides a mechanism for introducing measurement error into the stochastic process. It arises when considering a model of the form:

$$Z(\mathbf{X}) = m(\mathbf{X}, \beta) + \varepsilon(\mathbf{X}) + \eta(\mathbf{X}), \tag{2}$$

where $m(\cdot, \cdot)$ is underlying (usually linear) mean process, $\varepsilon(\cdot)$ is a process covariance whose underlying correlation is governed by K^*, and $\eta(\cdot)$ represents i.i.d. Gaussian noise. Secondarily, though perhaps of equal practical importance, the nugget (or jitter) prevents $\mathbf{K}$ from becoming numerically singular. Notational convenience and conceptual congruence motivates referral to $\mathbf{K}$ as a correlation matrix, even though the nugget term (g) forces $K(\mathbf{x}_i, \mathbf{x}_i) > 1$.

2.1.2 Exponential Power family

Correlation functions in the *isotropic power* family are *stationary* which means that correlations are measured identically throughout the input domain, and *isotropic* in that correlations $K^*(\mathbf{x}_j, \mathbf{x}_k)$ depend only on a function of the Euclidean distance between $\mathbf{x}_j$ and $\mathbf{x}_k$: $||\mathbf{x}_j - \mathbf{x}_k||$.

$$K^*_\nu(\mathbf{x}_j, \mathbf{x}_k | d_\nu) = \exp\left\{ -\frac{||\mathbf{x}_j - \mathbf{x}_k||^{p_0}}{d} \right\}, \tag{3}$$

where $d > 0$ is referred to as the *width* or *range* parameter. The power $0 < p_0 \leq 2$ determines the smoothness of the underlying process. A typical default choice is the Gaussian $p_0 = 2$ which gives an infinitely differentiable process.

A straightforward enhancement to the isotropic power family is to employ a unique range parameter d_i in each dimension ($i = 1, \ldots, m_X$). The resulting *separable* correlation function is still stationary, but no longer isotropic.

$$K^*(\mathbf{x}_j, \mathbf{x}_k | \mathbf{d}) = \exp\left\{ -\sum_{i=1}^{m_X} \frac{|x_{ij} - x_{ik}|^{p_0}}{d_i} \right\} \tag{4}$$

The isotropic power family is a special case (when $d_i = d$, for $i = 1, \ldots, m_X$). With the *separable power* family, one can model correlations in some input variables as stronger than others. However, with added flexibility comes added costs. When the true underlying correlation structure is isotropic, estimating the extra parameters of the separable model represents a sort of overkill.

2.1.3 Prediction and Adaptive Sampling

The predicted value of $z(\mathbf{x})$ is normally distributed with mean and variance

$$\hat{z}(\mathbf{x}) = \mathbf{f}^\top(\mathbf{x})\tilde{\boldsymbol{\beta}} + \mathbf{k}(\mathbf{x})^\top \mathbf{K}^{-1}(\mathbf{Z} - \mathbf{F}\tilde{\boldsymbol{\beta}}), \tag{5}$$

$$\hat{\sigma}^2(\mathbf{x}) = \sigma^2[\kappa(\mathbf{x}, \mathbf{x}) - \mathbf{q}^\top(\mathbf{x})\mathbf{C}^{-1}\mathbf{q}(\mathbf{x})], \tag{6}$$

where $\tilde{\boldsymbol{\beta}}$ is the posterior mean estimate of $\boldsymbol{\beta}$, and

$$\begin{aligned} \mathbf{C}^{-1} &= (\mathbf{K} + \mathbf{F}\mathbf{W}\mathbf{F}^\top/\tau^2)^{-1} \\ \mathbf{q}(\mathbf{x}) &= \mathbf{k}(\mathbf{x}) + \tau^2 \mathbf{F}\mathbf{W}\mathbf{f}(\mathbf{x}) \\ \kappa(\mathbf{x}, \mathbf{y}) &= K(\mathbf{x}, \mathbf{y}) + \tau^2 \mathbf{f}^\top(\mathbf{x})\mathbf{W}\mathbf{f}(\mathbf{y}) \end{aligned}$$

with $\mathbf{f}^\top(\mathbf{x}) = (1, \mathbf{x}^\top)$, and $\mathbf{k}(\mathbf{x})$ a $n-$vector with $\mathbf{k}_{\nu,j}(\mathbf{x}) = K(\mathbf{x}, \mathbf{x}_j)$, for all $\mathbf{x}_j \in \mathbf{X}$. Notice that $\hat{\sigma}(\mathbf{x})^2$ does not directly depend on the observed responses $\mathbf{Z}$. These equations often called *kirking* equations [16].

The ALM algorithm [15] is implemented with MCMC inference by computing the norm (or width) of predictive quantiles obtained by samples from the Normal distribution given above. The ALC algorithm [5] computes the reduction in variance given that the candidate location $\tilde{\mathbf{x}} \in \tilde{\mathbf{X}}$ is added into the data

(averaged over a reference set $\tilde{\mathbf{Y}}$):

$$\Delta\hat{\sigma}^2(\tilde{\mathbf{x}}) = \frac{1}{|\tilde{\mathbf{Y}}|}\sum_{\mathbf{y}\in\tilde{\mathbf{Y}}} \Delta\hat{\sigma}^2_{\mathbf{y}}(\tilde{\mathbf{x}}) = \frac{1}{|\tilde{\mathbf{Y}}|}\sum_{\mathbf{y}\in\tilde{\mathbf{Y}}} \hat{\sigma}^2_{\mathbf{y}} - \hat{\sigma}^2_{\mathbf{y}}(\tilde{\mathbf{x}}) \tag{7}$$
$$= \frac{1}{|\tilde{\mathbf{Y}}|}\sum_{\mathbf{y}\in\tilde{\mathbf{Y}}} \frac{\sigma^2\left[\mathbf{q}_N^\top(\mathbf{y})\mathbf{C}_N^{-1}\mathbf{q}_N(\tilde{\mathbf{x}}) - \kappa(\tilde{\mathbf{x}},\mathbf{y})\right]^2}{\kappa(\tilde{\mathbf{x}},\tilde{\mathbf{x}}) - \mathbf{q}_N^\top(\tilde{\mathbf{x}})\mathbf{C}_N^{-1}\mathbf{q}_N(\tilde{\mathbf{x}})},$$

which is easily computed using MCMC methods. In the `tgp` package, the reference set is taken to be the same as the candidate set, i.e., $\tilde{\mathbf{Y}} = \tilde{\mathbf{X}}$.

The Expected Global Optimization (EGO) algorithm [14] is centered around a statistic which captures the expected improvement in the model about its ability to predict the spatial location of its global minimum. If $f_{\min}$ is the model's current best guess about the minimum, e.g., $f_{\min} = \min\{z_1, \ldots, z_N\}$, then the expected improvement at the point $\tilde{\mathbf{x}}$ can reasonably be encoded as

$$E[I(\tilde{\mathbf{x}})] = E[\max(f_{\min} - Z(\tilde{\mathbf{x}}), 0)],$$

which can be shown to work out to be

$$E[I(\tilde{\mathbf{x}})] = (f_{\min} - \hat{z}(\tilde{\mathbf{x}}))\,\Phi\left(\frac{f_{\min} - \hat{z}(\tilde{\mathbf{x}})}{\hat{\sigma}^2(\tilde{\mathbf{x}})}\right) + \hat{\sigma}^2(\tilde{\mathbf{x}})\,\phi\left(\frac{f_{\min} - \hat{z}(\tilde{\mathbf{x}})}{\hat{\sigma}^2(\tilde{\mathbf{x}})}\right) \tag{8}$$

where $\hat{z}$ and $\hat{\sigma}^2$ are taken from the equations for the posterior predictive distribution (5). Φ and ϕ are the standard Normal cumulative distribution and probability density functions, respectively. MCMC samples from (8) can be gathered in order to determine which $\tilde{\mathbf{x}}$ of a candidate set of locations $\tilde{\mathbf{x}} \in \tilde{\mathbf{X}}$ give the highest reduction in uncertainty about the global minimum.

2.2 GPs and Limiting linear models

A special limiting case of the Gaussian process model is the standard linear model. Replacing the top (likelihood) line in the hierarchical model (1)

$$\mathbf{Z}|\boldsymbol{\beta}, \sigma^2, \mathbf{K} \sim N(\mathbf{F}\boldsymbol{\beta}, \sigma^2\mathbf{K}) \qquad \text{with} \qquad \mathbf{Z}|\boldsymbol{\beta}, \sigma^2 \sim N(\mathbf{F}\boldsymbol{\beta}, \sigma^2\mathbf{I}),$$

where $\mathbf{I}$ is the $n \times n$ identity matrix, gives a parameterization of a linear model. From a phenomenological perspective, GP regression is more flexible than standard linear regression in that it can capture nonlinearities in the interaction between covariates ($\mathbf{x}$) and responses (z). From a modeling perspective, the GP can be more than just overkill for linear data. Parsimony and over-fitting considerations are just the tip of the iceberg. It is also unnecessarily computationally expensive, as well as numerically unstable. Specifically, it requires the inversion of a large covariance matrix— an operation whose computing cost grows with the cube of the sample size. Moreover, large finite d parameters can be problematic from a numerical perspective because, unless g is also large, the resulting covariance matrix can be numerically singular when the off-diagonal elements of $\mathbf{K}$ are nearly one.

Bayesians can take advantage of the limiting linear model (LLM) by constructing prior for the "mixture" of the GP with its LLM [12, 10]. The key idea is an augmentation of the parameter space by m_X indicators $\mathbf{b} = \{b\}_{i=1}^{m_X} \in \{0,1\}^{m_X}$. The boolean b_i is intended to select either the GP ($b_i = 1$) or its LLM for the i^{th} dimension. The actual range parameter used by the correlation function is multiplied by $\mathbf{b}$: e.g. $K^*(\cdot,\cdot|\mathbf{b}^\top\mathbf{d})$. To encode the preference that GPs with larger range parameters be more likely to "jump" to the LLM, the prior on b_i is specified as a function of the range parameter d_i: $p(b_i, d_i) = p(b_i|d_i)p(d_i)$.

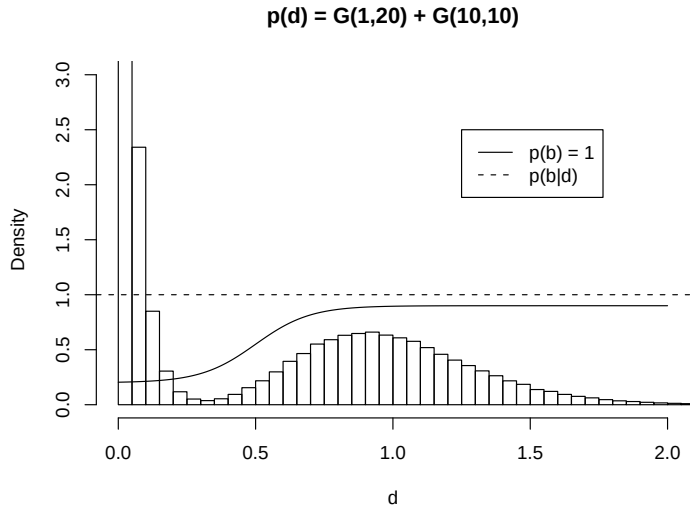

Figure 1: Prior distribution for the boolean (b) superimposed on $p(d)$.

Probability mass functions which increase as a function of d_i, e.g.,

$$p_{\gamma,\theta_1,\theta_2}(b_i = 0|d_i) = \theta_1 + (\theta_2 - \theta_1)/(1 + \exp\{-\gamma(d_i - 0.5)\}) \tag{9}$$

with $0 < \gamma$ and $0 \leq \theta_1 \leq \theta_2 < 1$, can encode such a preference by calling for the exclusion of dimensions i with with large d_i when constructing $\mathbf{K}^*$. Thus b_i determines whether the GP or the LLM is in charge of the marginal process in the i^{th} dimension. Accordingly, θ_1 and θ_2 represent minimum and maximum probabilities of jumping to the LLM, while γ governs the rate at which $p(b_i = 0|d_i)$ grows to θ_2 as d_i increases. Figure 1 plots $p(b_i = 0|d_i)$ for $(\gamma, \theta_1, \theta_2) = (10, 0.2, 0.95)$ superimposed on a convenient $p(d_i)$ which is taken to be a mixture of Gamma distributions,

$$p(d) = [G(d|\alpha = 1, \beta = 20) + G(d|\alpha = 10, \beta = 10)]/2, \tag{10}$$

representing a population of GP parameterizations for wavy surfaces (small d) and a separate population of those which are quite smooth or approximately

linear. The θ_2 parameter is taken to be strictly less than one so as not to preclude a GP which models a genuinely nonlinear surface using an uncommonly large range setting.

The implied prior probability of the full m_X-dimensional LLM is

$$p(\text{linear model}) = \prod_{i=1}^{m_X} p(b_i = 0|d_i) = \prod_{i=1}^{m_X} \left[\theta_1 + \frac{\theta_2 - \theta_1}{1 + \exp\{-\gamma(d_i - 0.5)\}}\right]. \quad (11)$$

Notice that the resulting process is still a GP if any of the booleans b_i are one. The primary computational advantage associated with the LLM is foregone unless all of the b_i's are zero. However, the intermediate result offers increased numerical stability and represents a unique transitionary model lying somewhere between the GP and the LLM. It allows for the implementation of semiparametric stochastic processes like $Z(\mathbf{x}) = \boldsymbol{\beta} f(\mathbf{x}) + \varepsilon(\tilde{\mathbf{x}})$ representing a piecemeal spatial extension of a simple linear model. The first part ($\boldsymbol{\beta} f(\mathbf{x})$) of the process is linear in some known function of the full set of covariates $\mathbf{x} = \{x_i\}_{i=1}^{m_X}$, and $\varepsilon(\cdot)$ is a spatial random process (e.g. a GP) which acts on a subset of the covariates $\tilde{\mathbf{x}}$. Such models are commonplace in the statistics community [7]. Traditionally, $\tilde{\mathbf{x}}$ is determined and fixed *a' priori*. The separable boolean prior (9) implements an adaptively semiparametric process where the subset $\tilde{\mathbf{x}} = \{x_i : b_i = 1, i = 1, \ldots, m_X\}$ is given a prior distribution, instead of being fixed.

2.2.1 Prediction and Adaptive Sampling under LLM

Prediction under the limiting GP model is a simplification of (5) when it is known that $\mathbf{K} = (1 + g)\mathbf{I}$. It can be shown [12, 10] that the predicted value of z at $\mathbf{x}$ is normally distributed with mean $\hat{z}(\mathbf{x}) = \mathbf{f}^\top(\mathbf{x})\tilde{\boldsymbol{\beta}}$ and variance $\hat{\sigma}(\mathbf{x})^2 = \sigma^2[1 + \mathbf{f}^\top(\mathbf{x})\mathbf{V}_{\tilde{\beta}}\mathbf{f}(\mathbf{x})]$, where $\mathbf{V}_{\tilde{\beta}} = (\tau^{-2} + \mathbf{F}^\top\mathbf{F}(1+g))^{-1}$. This is preferred over (5) with $\mathbf{K} = \mathbf{I}(1 + g)$ because an $m_X \times m_X$ inversion is faster than an $n \times n$ one.

Applying the ALC algorithm under the LLM is computationally less intense compared to ALC under a full GP. Starting with the predictive variance given in (5), the expected reduction in variance under the LM is [10]

$$\Delta\hat{\sigma}^2_{\mathbf{y}}(\mathbf{x}) = \frac{\sigma^2[\mathbf{f}^\top(\mathbf{y})\mathbf{V}_{\tilde{\beta}_N}\mathbf{f}(\mathbf{x})]^2}{1 + g + \mathbf{f}^\top(\mathbf{x})\mathbf{V}_{\tilde{\beta}_N}\mathbf{f}(\mathbf{x})}. \quad (12)$$

Since only an $m_X \times m_X$ inverse is required, Eq. (12) is preferred over simply replacing $\mathbf{K}$ with $\mathbf{I}(1 + g)$ in (7), which requires an $n \times n$ inverse.

The statistic for the EGO algorithm is the same under the LLM as (8) for the GP. Of course, it helps to use the linear predictive equations instead of the kriging ones for $\hat{z}(\mathbf{x})$ and $\hat{\sigma}^2(\mathbf{x})$.

2.3 Treed partitioning

Nonstationary models are obtained by treed partitioning and inferring a separate model within each region of the partition. Treed partitioning is accomplished

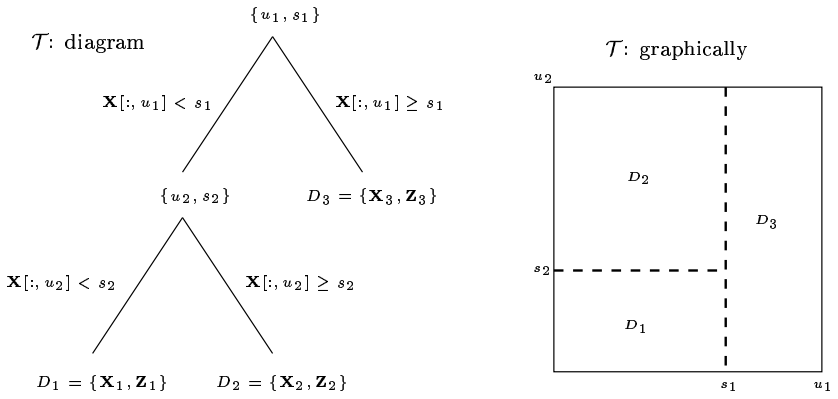

Figure 2: An example tree $\mathcal{T}$ with two splits, resulting in three regions, shown in a diagram (*left*) and pictorially (*left*).

by making (recursive) binary splits on the value of a single variable so that region boundaries are parallel to coordinate axes. Partitioning is recursive, so each new partition is a sub-partition of a previous one. Since variables may be revisited, there is no loss of generality by using binary splits as multiple splits on the same variable are equivalent to a non-binary split.

Figure 2 shows an example tree. In this example, region D_1 contains $\mathbf{x}$'s whose u_1 coordinate is less than s_1 and whose u_2 coordinate is less than s_2. Like D_1, D_2 has $\mathbf{x}$'s whose coordinate u_1 is less than s_1, but differs from D_1 in that the u_2 coordinate must be bigger than or equal to s_2. Finally, D_3 contains the rest of the $\mathbf{x}$'s differing from those in D_1 and D_2 because the u_1 coordinate of its $\mathbf{x}$'s is greater than or equal to s_1. The corresponding response values (z) accompany the $\mathbf{x}$'s of each region.

These sorts of models are often referred to as Classification and Regression Trees (CART) [1]. CART has become popular because of its ease of use, clear interpretation, and ability to provide a good fit in many cases. The Bayesian approach is straightforward to apply to tree models, provided that one can specify a meaningful prior for the size of the tree. The tree process implemented in the `tgp` package follows Chipman et al. [3] who specify the prior through a tree-generating process. Starting with a null tree (all data in a single partition), the tree, $\mathcal{T}$, is probabilistically split recursively with each partition, η, being split with probability $p_{\text{SPLIT}}(\eta, \mathcal{T}) = a(1 + q_\eta)^{-b}$ where q_η is the depth of η in $\mathcal{T}$ and a and b are parameters chosen to give an appropriate size and spread to the distribution of trees.

Extending the work of Chipman et al. [4], the `tgp` package implements a stationary GP with linear trend, or GP LLM, independently within each of the regions depicted by a tree $\mathcal{T}$. Integrating out dependence on $\mathcal{T}$ is accomplished by reversible-jump MCMC (RJ-MCMC) via tree operations *grow, prune, change*, and *swap* [3]. To keep things simple, proposals for new parameters—via

an increase in the number of partitions—are drawn from their priors, thus eliminating the Jacobian term usually present in RJ-MCMC. New splits are chosen uniformly from the set of marginalized input locations $\mathbf{X}$. The *swap* operation is augmented with a *rotate* option to improve mixing of the Markov chain [10].

There are many advantages to partitioning the input space into regions, and fitting separate GPs (or GP LLMs) within each region. Partitioning allows for the modeling of non-stationary behavior, and can ameliorate some of the computational demands by fitting models to less data. Finally, a fully Bayesian approach yields a uniquely efficient nonstationary, nonparametric, or semiparametric (in the case of the GP LLM) regression tool.

2.4 (Treed) sequential D-optimal design

In the statistics community, the traditional approach to sequential data solicitation goes under the general heading of *(Sequential) Design of Experiments* [20]. Depending on a choice of utility, different algorithms for obtaining optimal designs can be derived. For example, one can choose the Kullback-Leibler distance between the posterior and prior distributions as a utility. For Gaussian process models with correlation matrix $\mathbf{K}$, this is equivalent to maximizing $\det(\mathbf{K})$. Subsequently chosen input configurations are called $D-$optimal designs. Choosing quadratic loss leads to what are called $A-$optimal designs. An excellent review of Bayesian approaches to the design of experiments is provided by Chaloner & Verdinelli [2].

Other approaches used by the statistics community include space-filling designs: e.g. max-min distance and Latin Hypercube (LH) designs [20]. The `FIELDS` package [8], available from CRAN, implements code for space-filling designs in addition to kriging and thin plate spline models for spatial interpolation.

A hybrid approach to designing experiments employs active learning techniques. The idea is to choose a set of candidate input configurations $\tilde{\mathbf{X}}$ (say, a $D-$optimal or LH design) and an active learning rule for determining the order in which they are be added into the design. The ALM algorithm has been shown to approximate maximum expected information designs by selecting the candidate location $\tilde{\mathbf{x}} \in \tilde{\mathbf{X}}$ which has the greatest standard deviation in predicted output [15]. An alternative algorithm is to select $\tilde{\mathbf{x}}$ minimizing the resulting expected squared error averaged over the input space [5], called ALC for Active Learning–Cohn. Seo et al. [21] provide a comparison between ALC and ALM using standard GPs. The EGO [14] algorithm can be used to find global minima.

Choosing candidate configurations $\tilde{\mathbf{X}}$ (`XX` in the `tgp` package), at which to gather ALM, ALC, or EGO statistics, is half of the challenge in the hybrid approach to experimental design. Arranging candidates so that they are well-spaced out relative to themselves, and relative to already sampled configurations, is clearly desirable. Towards this end, a sequential D-optimal design is a good first choice. However, traditional D-optimal designs fall short of the task for a number of reasons. They are based on a *known* parameterization of a single GP model, and are thus not well-suited to MCMC inference. A D-

optimal design may not choose candidates in the "interesting" part of the input space, because sampling is high there already. Classic optimal design criteria, in general, are ill-suited partition models wherein "closeness" may not measured homogeneously across the input space. Another disadvantage is computational, namely decomposing and finding the determinant of a large covariance matrix.

One possible solution to both computational and nonstationary modeling issues is to use treed sequential D-optimal design [10]. Separate sequential D-optimal designs can be computed in each of the partitions depicted by the maximum *a posteriori* (MAP) tree $\hat{\mathcal{T}}$. The number of candidates selected from each region can be proportional to the volume of—or proportional to the number of grid locations in—the region. MAP parameters $\hat{\boldsymbol{\theta}}_\nu|\hat{\mathcal{T}}$, or "neutral" or "exploration encouraging" ones, can be used to create the candidate design. Separating design from inference by using custom parameterizations in design steps, rather than inferred ones, is a common practice [20]. Small range parameters, for learning about the wiggliness of the response, and a modest nugget parameter, for numerical stability, tend to work well together.

Finding a local maxima is generally sufficient to get well-spaced candidates. The `dopt.gp` function uses a stochastic ascent algorithm which can find local maxima without calculating too many determinants.

3 Examples using `tgp`

The following subsections take the reader through a series of examples based, mostly, on synthetic data. At least two different `b*` models are fit for each set of data, offering comparisons and contrasts. Duplicating these examples in your own `R` session is highly recommended. The `Stangle` function can help extract executable `R` code from this document. For example, the code for the exponential data of Section 3.3 can be extracted with one command.

```
> Stangle(vignette("exp", package="tgp")$file))
```

This will write a file called "exp.R". Additionally, each of the subsections that follow is available as an `R` demo. Try `demo(package="tgp")` for a listing of available demos. To envoke the demo for the exponential data of Section 3.3 try `demo(exp, package="tgp")`. This is equivalent to `source("exp.R")` because the demos were created using `Stangle` on the source files of this document.

Other successful uses of the methods in this pacakge include applications to the Boston housing data [13], and designing an experiment for a reusable NASA launch vehicle [11, 10] called the Langely glide-back booster (LGBB).

3.1 1-d Linear data

Consider data sampled from a linear model.

$$z_i = 1 + 2x_i + \epsilon, \quad \text{where} \quad \epsilon_i \overset{\text{iid}}{\sim} N(0, 0.25^2) \tag{13}$$

The following R code takes a sample $\{\mathbf{X}, \mathbf{Z}\}$ of size $N = 50$ from (13). It also chooses $N' = 99$ evenly spaced predictive locations $\tilde{\mathbf{X}} =$ XX.

```
> X <- seq(0, 1, length = 50)
> XX <- seq(0, 1, length = 99)
> Z <- 1 + 2 * X + rnorm(length(X), sd = 0.25)
```

Using tgp on this data with a Bayesian hierarchical linear model goes as follows:

```
> lin.blm <- blm(X = X, XX = XX, Z = Z)

n=50, d=1, nn=99
BTE=(1000,4000,3), R=1, linburn=0
preds: data
tree[alpha,beta,nmin]=[0,0,10]
linear prior: flat
s2[a0,g0]=[5,10]
s2 lambda[a0,g0]=[0.2,10]
corr prior: separable power
nug[a,b][0,1]=[1,1],[1,1]
nug prior fixed
gamlin=[-1,0.2,0.7]
d[a,b][0]=[1,20],[10,20]
d prior fixed

burn in:
r=1000 corr=[0] : n = 50

Obtaining samples (nn=99 predictive locations):
r=1000 corr=[0] : mh=1 n = 50
r=2000 corr=[0] : mh=1 n = 50
r=3000 corr=[0] : mh=1 n = 50

finished repetition 1 of 1
removed 0 leaves from the tree
```

The first group of text printed to stdout is a summary of inputs to the C code, and the prior parameterization. Then, MCMC progress indicators are printed every 1,000 rounds. The linear model is indicated by cor=[0]. In terminal versions, e.g. Unix, the progress indicators can give a sense of when the code will finish. GUI versions of R—Windows or MacOS X—usually buffer stdout, rendering this feature essentially useless as a real-time indicator of progress. Note that a user cannot interact with R while the C code is running. This will be changed in future versions.

The generic plot method can be used to visualize the fitted posterior predictive surface (with option layout = 'surf') in terms of means and credible

```
> plot(lin.blm, main = "Linear Model,", layout = "surf")
> abline(1, 2, lty = 3, col = "blue")
```

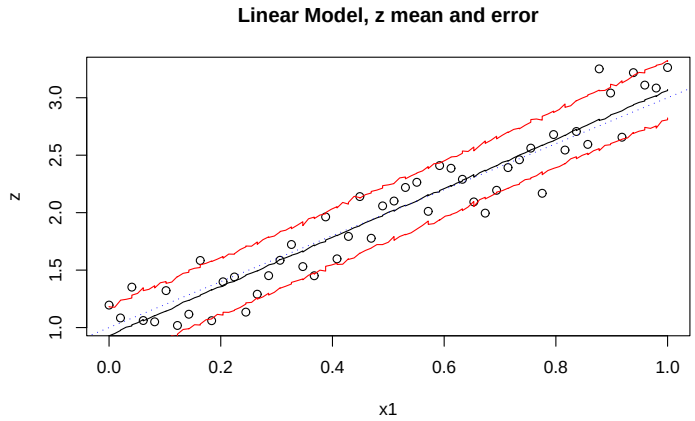

Figure 3: Posterior predictive distribution using `blm` on synthetic linear data: mean and 90% credible interval. The actual generating lines are shown as blue-dotted.

intervals. Figure 3 shows how to do it, and what you get. The default option `layout = 'both'` shows both a predictive surface and error (or uncertainty) plot, side by side. The error plot can be obtained alone via `layout = 'as'`. Examples of these layouts appear later.

If, say, you were unsure about the dubious "linearness" of this data, you might try a GP LLM (using `btgpllm`) and let a more flexible model speak as to the linearity of the process.

```
> lin.gpllm <- bgpllm(X = X, XX = XX, Z = Z)

n=50, d=1, nn=99
BTE=(1000,4000,2), R=1, linburn=0
preds: data
tree[alpha,beta,nmin]=[0,0,10]
linear prior: flat
s2[a0,g0]=[5,10]
s2 lambda[a0,g0]=[0.2,10]
corr prior: separable power
nug[a,b][0,1]=[1,1],[1,1]
nug prior fixed
gamlin=[10,0.2,0.7]
d[a,b][0]=[1,20],[10,20]
d prior fixed

burn in:
r=1000 corr=[0] : n = 50
```

```
Obtaining samples (nn=99 predictive locations):
r=1000 corr=[0] : mh=1 n = 50
r=2000 corr=[0] : mh=1 n = 50
r=3000 corr=[0] : mh=1 n = 50

finished repetition 1 of 1
removed 0 leaves from the tree

> plot(lin.gpllm, main = "GP LLM,", layout = "surf")
> abline(1, 2, lty = 4, col = "blue")
```

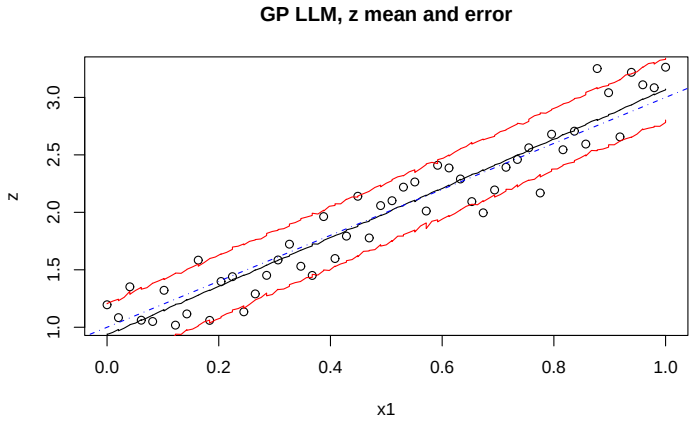

Figure 4: Posterior predictive distribution using `bgpllm` on synthetic linear data: mean and 90% credible interval. The actual generating lines are shown as blue-dotted.

Whenever the progress indicators show `corr[0]` the process is under the LLM in that round, and the GP otherwise. A plot of the resulting surface is shown in Figure 4 for comparison. Since the data is linear, the resulting predictive surfaces should look strikingly similar to one another. On occasion, the GP LLM may find some bendy-ness in the surface. This happens rarely with samples as large as $N = 50$, but is quite a bit more common for $N < 20$.

3.2 1-d Synthetic Sine Data

Consider 1-dimensional simulated data which is partly a mixture of sines and cosines, and partly linear.

$$z(x) = \begin{cases} \sin\left(\frac{\pi x}{5}\right) + \frac{1}{5}\cos\left(\frac{4\pi x}{5}\right) & x < 10 \\ x/10 - 1 & \text{otherwise} \end{cases} \tag{14}$$

The `R` code below obtains $N = 100$ evenly spaced samples from this data in the domain $[0, 20]$, with noise added to keep things interesting. Some evenly spaced predictive locations `XX` are also created.

```
> X <- seq(0, 20, length = 100)
> XX <- seq(0, 20, length = 99)
> Z <- (sin(pi * X/5) + 0.2 * cos(4 * pi * X/5)) *
+     (X <= 9.6)
> lin <- X > 9.6
> Z[lin] <- -1 + X[lin]/10
> Z <- Z + rnorm(length(Z), sd = 0.1)
```

By design, the data is clearly nonstationary. Perhaps not knowing this, good first model choice for this data might be a GP.

```
> sin.bgp <- bgp(X = X, Z = Z, XX = XX)
```

```
> plot(sin.bgp, main = "GP,", layout = "surf")
```

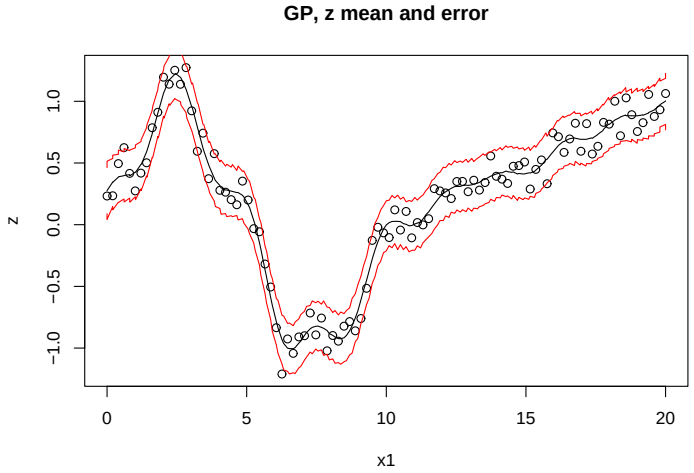

Figure 5: Posterior predictive distribution using **bgp** on synthetic sinusoidal data: mean and 90% credible interval

Progress indicators have been suppressed. Figure 5 shows the resulting posterior predictive surface under the GP. Notice how the (stationary) GP gets the wiggliness of the sinusoidal region, but fails to capture the smoothness of the linear region. This is becuase the data comes from a process that is nonstationary.

So one might consider a Bayesian CART model instead.

```
> sin.btlm <- btlm(X = X, Z = Z, XX = XX)
```

```
n=100, d=1, nn=99
BTE=(2000,7000,2), R=1, linburn=0
preds: data
tree[alpha,beta,nmin]=[0.25,2,10]
linear prior: flat
```

```
s2[a0,g0]=[5,10]
s2 lambda[a0,g0]=[0.2,10]
corr prior: separable power
nug[a,b][0,1]=[1,1],[1,1]
nug prior fixed
gamlin=[-1,0.2,0.7]
d[a,b][0]=[1,20],[10,20]
d prior fixed

burn in:
**GROW** @depth 0: [0,0.494949], n=(50,50)
**GROW** @depth 1: [0,0.20202], n=(21,29)
**GROW** @depth 1: [0,0.10101], n=(11,10)
**GROW** @depth 3: [0,0.353535], n=(11,11)
r=1000 corr=[0] [0] [0] [0] [0] : n = 10 14 10 13 53
**PRUNE** @depth 3: [0,0.222222]
r=2000 corr=[0] [0] [0] [0] : n = 10 20 17 53

Obtaining samples (nn=99 predictive locations):
r=1000 corr=[0] [0] [0] [0] : mh=4 n = 10 21 16 53
r=2000 corr=[0] [0] [0] [0] : mh=4 n = 15 15 17 53
r=3000 corr=[0] [0] [0] [0] : mh=4 n = 15 15 17 53
r=4000 corr=[0] [0] [0] [0] : mh=4 n = 15 15 17 53
r=5000 corr=[0] [0] [0] [0] : mh=4 n = 16 14 17 53
Grow: 0.01072%, Prune: 0.002899%, Change: 0.1496%, Swap: 0.7925%

finished repetition 1 of 1
removed 4 leaves from the tree
```

MCMC progress indicators printed to `stdout` indicate successful *grow* and *prune* operations as they happen, and region sizes n every 1,000 rounds.

Figure 6 shows the resulting posterior predictive surface (*top*) and trees (*bottom*). The MAP partition ($\hat{\mathcal{T}}$) is also drawn onto the surface plot (*top*) in the form of vertical lines. The CART model captures the smoothness of the linear region just fine, but comes up short in the sinusoidal region—doing the best it can with piecewise linear models.

The ideal model for this data is the Bayesian treed GP becuase it can be both smooth and wiggly.

```
> sin.btgp <- btgp(X = X, Z = Z, XX = XX)
```

Progress indicators have been suppressed. Figure 7 shows the resulting posterior predictive surface (*top*) and trees (*bottom*).

Finally, speedups can be obtained if the GP is allowed to jump to the LLM [10], since half of the response surface is *very* smooth, or linear. This is not shown here since the results are very similar to those above, replacing `btgp`

```
> plot(sin.btlm, main = "Linear CART,", layout = "surf")
```

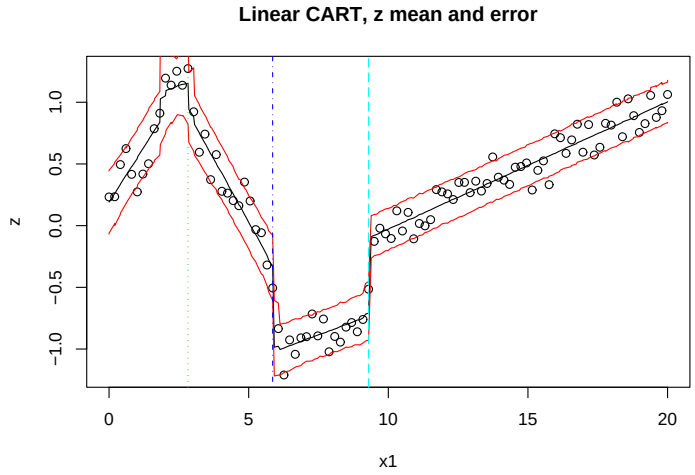


```
> tgp.trees(sin.btlm)
```

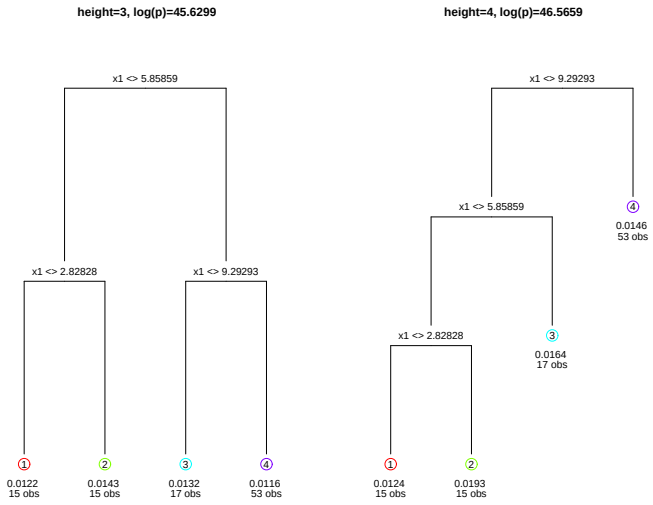

Figure 6: *Top:* Posterior predictive distribution using `btlm` on synthetic sinusoidal data: mean and 90% credible interval, and MAP partition ($\hat{T}$); *Bottom* MAP trees for each height encountered in the Markov chain showing $\hat{\sigma}^2$ and the number of observation n, at each leaf.

with `btgpllm`. The example in the next subsection offers a comparison for 2-d data.

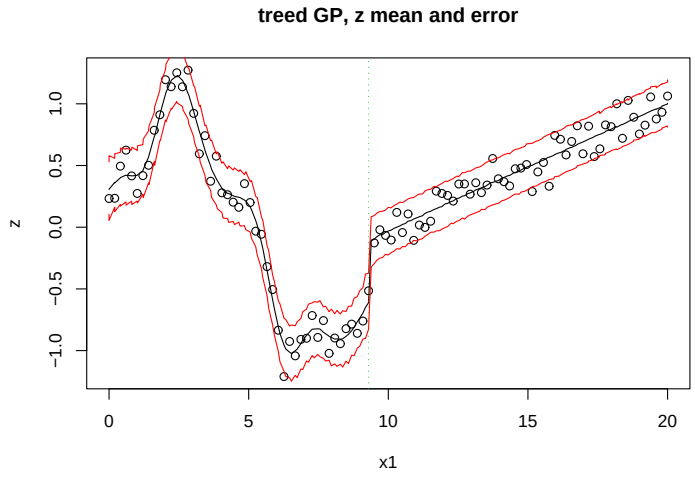


```
> tgp.trees(sin.btgp)
```

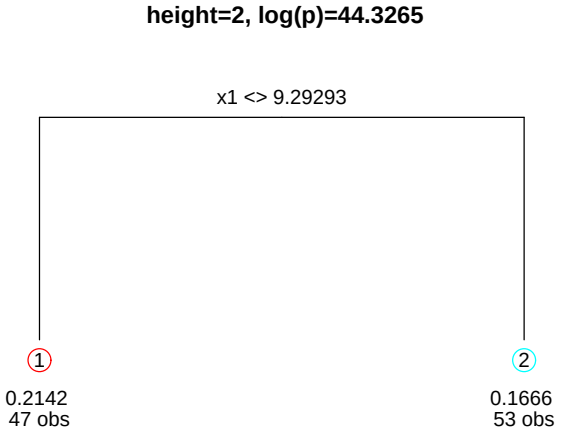

Figure 7: *Top:* Posterior predictive distribution using `btgp` on synthetic sinusoidal data: mean and 90% credible interval, and MAP partition ($\hat{T}$); *Bottom* MAP trees for each height encountered in the Markov chain.

3.3 Synthetic 2-d Exponential Data

The next example involves a two-dimensional input space in $[-2, 6] \times [-2, 6]$. The true response is given by

$$z(\mathbf{x}) = x_1 \exp(-x_1^2 - x_2^2). \tag{15}$$

A small amount of Gaussian noise (with sd = 0.001) is added. Besides its dimensionality, a key difference between this data set and the last one is that it is not defined using step functions; this smooth function does not have any artificial breaks between regions. The `tgp` package provides a function for data subsampled from a grid of inputs and outputs described by (15) which concentrates inputs (`X`) more heavily in the first quadrant where the response is more interesting. Predictive locations (`XX`) are the remaining grid locations.

```
> exp2d.data <- exp2d.rand()
> X <- exp2d.data$X
> Z <- exp2d.data$Z
> XX <- exp2d.data$XX
```

Linear CART is clearly just as inappropriate for this data as it was for the sinusoidal data in the previous section. However, a stationary GP fits this data just fine. After all, the process is quite well behaved. In two dimensions one has a choice between the isotropic and separable correlation functions. Separable is the default in the `tgp` package. For illustrative purposes here, I shall use the isotropic power family.

```
> exp.bgp <- bgp(X = X, Z = Z, XX = XX, corr = "exp")
```

```
> plot(exp.bgp, main = "GP,")
```

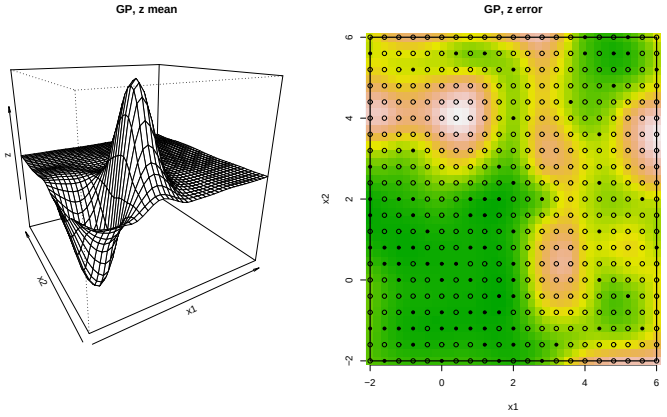

Figure 8: *Left:* posterior predictive mean using `bgp` on synthetic exponential data; *right* image plot of posterior predictive variance with data locations `X` (dots) and predictive locations `XX` (circles).

Progress indicators are suppressed. Figure 8 shows the resulting posterior predictive surface under the GP in terms of means (*left*) and variances (*right*) in the default layout. The sampled locations (`X`) are shown as dots on the *right* image plot. Predictive locations (`XX`) are circles. Predictive uncertainty for the stationary GP model is highest where sampling is lowest, despite that the process is very uninteresting there.

A treed GP seems more appropriate for this data. It can separate out the large uninteresting oart of the input space from the interesting part. The result is speedier inference and region-specific estimates of predictive uncertainty.

```
> exp.btgp <- btgp(X = X, Z = Z, XX = XX, corr = "exp")
```

```
> plot(exp.btgp, main = "treed GP,")
```

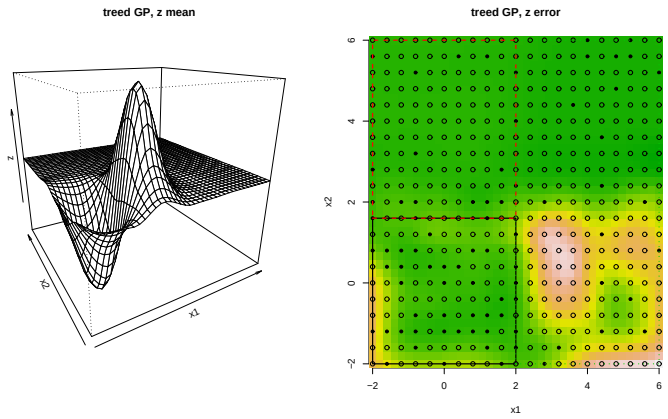


```
> tgp.trees(exp.btgp)
```

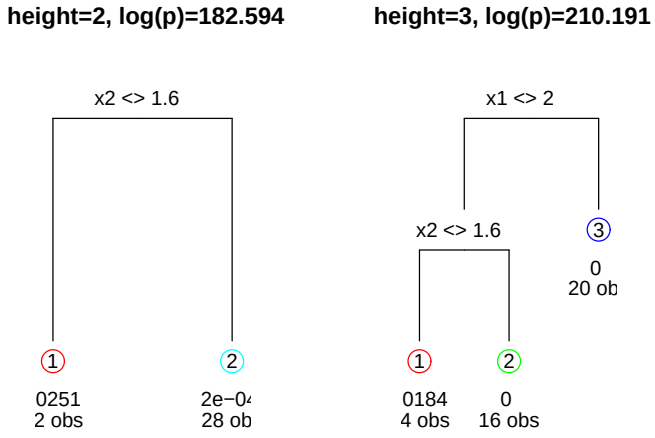

Figure 9: *Top-Left:* posterior predictive mean using `btgp` on synthetic exponential data; *top-right* image plot of posterior predictive variance with data locations `X` (dots) and predictive locations `XX` (circles). `Bottom:` MAP trees of each height encountered in the Markov chain with $\hat{\sigma}^2$ and the number of observations n at the leaves.

Figure 9 shows the resulting posterior predictive surface (*top*) and trees (*bottom*). Typical runs of the treed GP on this data find two, and if lucky three, partitions. As might be expected, jumping to the LLM for the uninteresting, zero-response, part of the input space can yield even further speedups [10]. Also, Chipman et al. recommend restarting the Markov chain a few times in order to better explore the marginal posterior for $\mathcal{T}$ [4]. This can be important for higher dimensional inputs requiring deeper trees. The `tgp` default is `R = 1`, i.e., one chain with no restarts. Here two chains—one restart—are obtained using `R = 2`.

```
> exp.btgpllm <- btgpllm(X = X, Z = Z, XX = XX, corr = "exp",
+     R = 2)

n=80, d=2, nn=361
BTE=(2000,7000,2), R=2, linburn=0
preds: data
tree[alpha,beta,minpart]=[0.25,2,10]
linear prior: flat
s2[a0,g0]=[5,10]
s2 lambda[a0,g0]=[0.2,10]
corr prior: isotropic power
nug[a,b][0,1]=[1,1],[1,1]
nug prior fixed
gamlin=[10,0.2,0.7]
d[a,b][0,1]=[1,20],[10,10]
d prior fixed

burn in:
**GROW** @depth 0: [1,0.35], n=(45,35)
**PRUNE** @depth 0: [1,0.4]
r=1000 corr=0.018638 : n = 80
**GROW** @depth 0: [0,0.5], n=(60,20)
r=2000 corr=0.0206168 0.114274 : n = 60 20

Obtaining samples (nn=361 predictive locations):
**GROW** @depth 1: [1,0.5], n=(50,10)
r=1000 corr=0.0226481 0(0.84922) 0(0.602632) : mh=3 n = 50 10 20
r=2000 corr=0.0230381 0(0.770479) 0.965604 : mh=3 n = 44 16 20
r=3000 corr=0.0209883 0(1.25422) 0(0.681911) : mh=3 n = 50 10 20
r=4000 corr=0.019928 0.785746 0.0729928 : mh=3 n = 44 16 20
r=5000 corr=0.0198103 0.813851 0.854068 : mh=3 n = 44 16 20
Grow: 0.008333%, Prune: 0.003597%, Change: 0.04887%, Swap: 0.178%

finished repetition 1 of 2
removed 3 leaves from the tree

burn in:
**GROW** @depth 0: [0,0.5], n=(60,20)
```

```
**GROW** @depth 1: [0,0.1], n=(15,36)
**PRUNE** @depth 1: [0,0.05]
**GROW** @depth 1: [1,0.5], n=(50,10)
r=1000 corr=0.0210184 0.0147621 0.94543 : mh=3 n = 44 16 20
r=2000 corr=0.0247164 0.0838776 1.39391 : mh=3 n = 44 16 20

Obtaining samples (nn=361 predictive locations):
r=1000 corr=0.0211024 1.32905 1.41035 : mh=3 n = 44 16 20
r=2000 corr=0.0203233 0(1.2382) 0(0.0643748) : mh=3 n = 50 10 20
r=3000 corr=0.021733 0(0.625732) 0.0239015 : mh=3 n = 50 10 20
r=4000 corr=0.0213785 0.0360728 0.108831 : mh=3 n = 44 16 20
r=5000 corr=0.0201093 0.0127475 0.0738182 : mh=3 n = 44 16 20
Grow: 0.007979%, Prune: 0.003356%, Change: 0.04622%, Swap: 0.1706%

finished repetition 2 of 2
removed 3 leaves from the tree


> plot(exp.btgpllm, main = "treed GP LLM,")
```

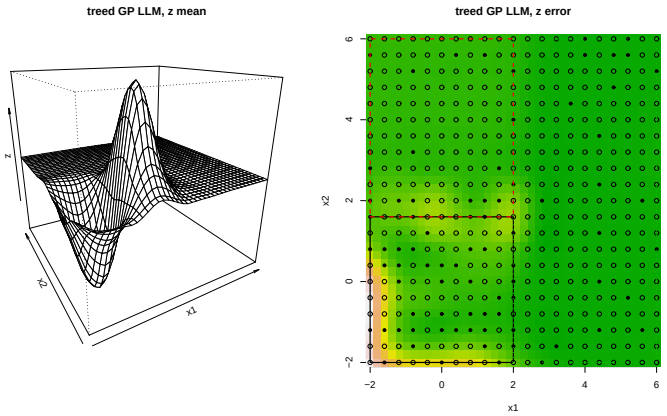

Figure 10: *Left:* posterior predictive mean using `btgpllm` on synthetic exponential data; *right* image plot of posterior predictive variance with data locations `X` (dots) and predictive locations `XX` (circles).

Progress indicators show where the LLM (`corr=0(`d`)`) or the GP is active. Figure 10 show how similar the resulting posterior predictive surfaces are compared to the treed GP (without LLM).

Finally, viewing 1-d projections of `tgp`-class output is possible by supplying a 1-vector `proj` argument to the `plot.tgp`. Figure 11 shows the two projections for `exp.btgpllm`. In the *left* surface plots the open circles indicate the mean of posterior priedictive distribution. Red lines show the 90% intervals, the norm of which are shown on the *right*.

```
> plot(exp.btgpllm, main = "treed GP LLM,", proj = c(1))
```

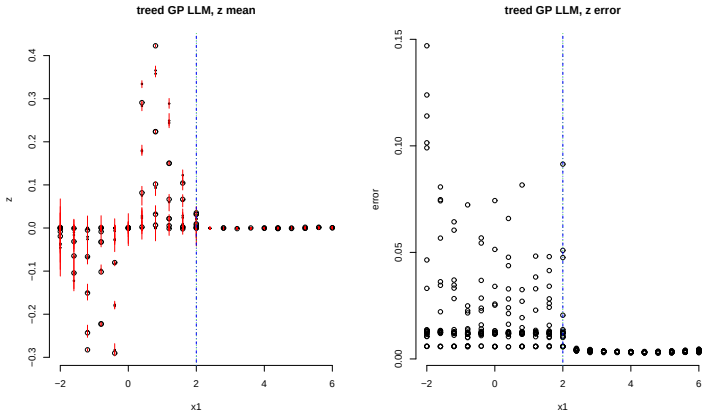


```
> plot(exp.btgpllm, main = "treed GP LLM,", proj = c(2))
```

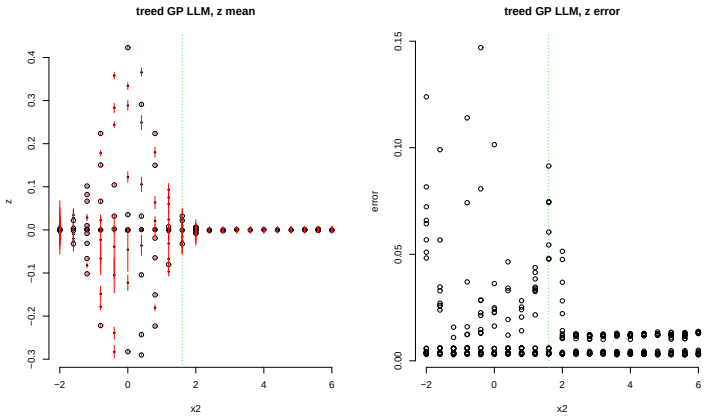

Figure 11: 1-d projections of the posterior predictive surface (*left*) and normed predictive intervals (*right*) of the 1-d tree GP LLM analysis of the synthetic exponential data. The *top* plots show projection onto the first input, and the *bottom* ones show the second.

3.4 Motorcycle Accident Data

The Motorcycle Accident Dataset [22] is a classic nonstationary data set used in recent literature [19] to demonstrate the success of nonstationary models. The data consists of measurements of the acceleration of the head of a motorcycle rider as a function of time in the first moments after an impact. In addition to being nonstationary, the data has input-dependent noise which makes it useful for illustrating how the treed GP model handles this nuance. There are at least two—perhaps three—three regions where the response exhibits different

behavior both in terms of the correlation structure and noise level.

The data is included as part of the `MASS` library in `R`.

```
> library(MASS)
```

Figure 12 shows how a stationary GP is able to capture the nonlinearity in the response but fails to capture the input dependent noise and increased smoothness (perhaps linearity) in parts of the input space.

```
> moto.bgp <- bgp(X = mcycle[, 1], Z = mcycle[, 2],
+     m0r1 = TRUE)
```

Since the responses in this data have a wide range, it helps to translate and rescale them so that they have a mean of zero and a range of one. The `m0r1` argument to `b*` and `tgp` functions automates this procedure. Progress indicators are surpressed.

```
> plot(moto.bgp, main = "GP,", layout = "surf")
```

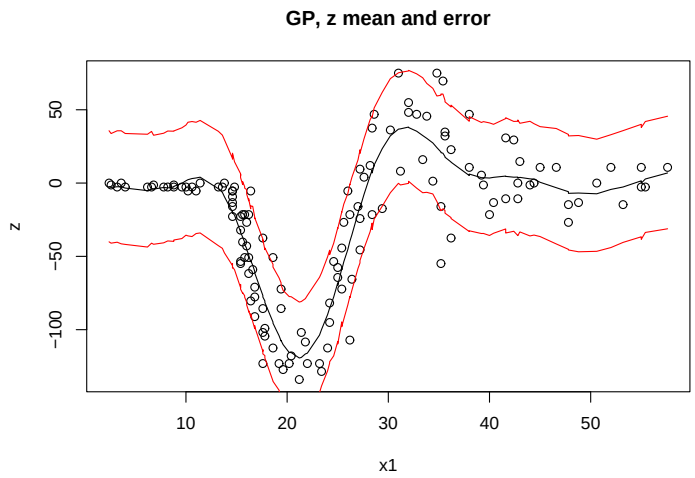

Figure 12: Posterior predictive distribution using `bgp` on the motorcycle accident data: mean and 90% credible interval

A Bayesian Linear CART model is able to capture the input dependent noise but fails to capture the waviness of the "whiplash"—center— segment of th the response.

```
> moto.btlm <- btlm(X = mcycle[, 1], Z = mcycle[, 2],
+     m0r1 = TRUE)
```

Figure 13 shows the resulting piecewise linear predictive surface and MAP partition ($\hat{T}$).

A treed GP model seems appropriate because it can model input dependent smoothness *and* noise. A treed GP LLM is probably most appropriate since the

```
> plot(moto.btlm, main = "Bayesian CART,", layout = "surf")
```

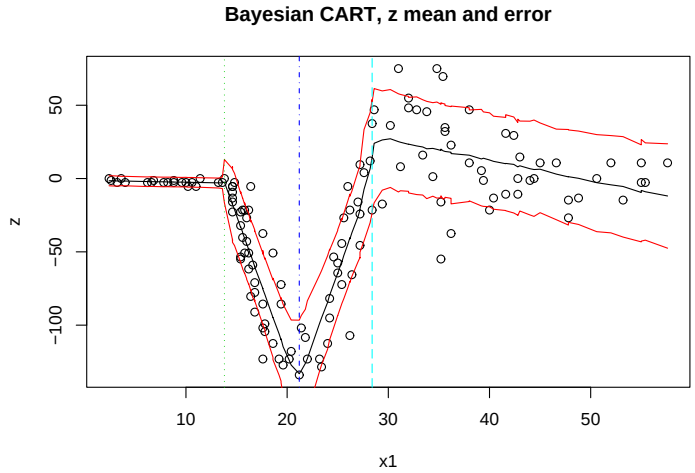

Figure 13: Posterior predictive distribution using `btlm` on the motorcycle accident data: mean and 90% credible interval

left-hand part of the input space is likely linear. One might further hypothesize that the right-hand region is also linear, perhaps with the same mean as the left-hand region, only with higher noise. The `b*` and `tgp` functions can force an i.i.d. hierarchical linear model by setting `bprior=b0`. Moreover, instead of rescaling the responses with `m0r1`, one might try encoding a mixture prior for the nugget in order to explicitly model region-specific noise. This requires direct usage of `tgp`.

```
> p <- tgp.default.params(2)
> p$bprior <- "b0"
> p$nug.p <- c(1, 0.1, 10, 0.1)
> moto.tgp <- tgp(X = mcycle[, 1], Z = mcycle[, 2],
+     params = p, BTE = c(2000, 22000, 2))
```

The resulting posterior predictive surface is shown in the *top* half of Figure 14. The *bottom* half of the figure shows the norm (difference) in predictive quantiles, clearly illustrating the treed GP's ability to capture input-specific noise in the posterior predictive distribution.

3.5 Friedman data

This Friedman data set is the first one of a suite that was used to illustrate MARS (Multivariate Adaptive Regression Splines) [9]. There are 10 covariates in the data ($\mathbf{x} = \{x_1, x_2, \ldots, x_{10}\}$). The function that describes the responses (Z), observed with standard Normal noise, has mean

$$E(Z|\mathbf{x}) = \mu = 10\sin(\pi x_1 x_2) + 20(x_3 - 0.5)^2 + 10x_4 + 5x_5, \qquad (16)$$

```
> plot(moto.tgp, main = "custom treed GP LLM,", layout = "surf")
```

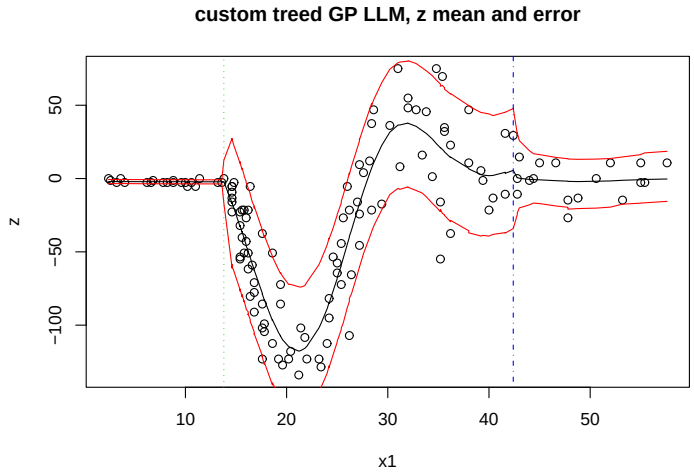


```
> plot(moto.tgp, main = "custom treed GP LLM,", layout = "as")
```

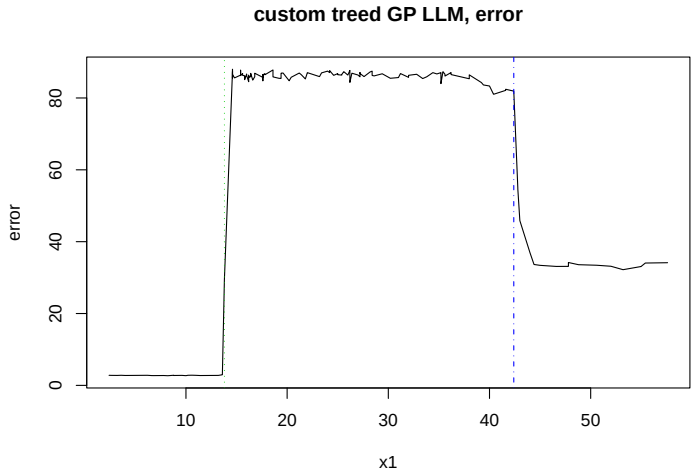

Figure 14: *top* Posterior predictive distribution using a custom parameterized `tgp` call on the motorcycle accident data: mean and 90% credible interval; *bottom* Quantile-norm (90%-5%) showing input-dependent noise.

but depends only on $\{x_1, \ldots, x_5\}$, thus combining nonlinear, linear, and irrelevant effects. Comparisons are made on this data to results provided for several other models in recent literature. Chipman et al. [4] used this data to compare their linear CART algorithm to four other methods of varying parameterization: linear regression, greedy tree, MARS, and neural networks. The statistic they

use for comparison is root mean-square error (RMSE)

$$\text{MSE} = \sum_{i=1}^{n} (\mu_i - \hat{z}_i)^2/n \qquad\qquad \text{RMSE} = \sqrt{\text{MSE}}$$

where $\hat{z}_i$ is the model-predicted response for input $\mathbf{x}_i$. The $\mathbf{x}$'s are randomly distributed on the unit interval.

Input data, responses, and predictive locations of size $N = 200$ and $N' = 1000$, respectively, can be obtained by a function included in the `tgp` package.

```
> f <- friedman.1.data(200)
> ff <- friedman.1.data(1000)
> X <- f[, 1:10]
> Z <- f$Y
> XX <- ff[, 1:10]
```

This example compares Bayesian linear CART with Bayesian GP LLM (not treed), following the RMSE experiments of Chipman et al. It helps to scale the responses so that they have a mean of zero and a range of one. First, fit the Bayesian linear CART model, and obtain the RMSE.

```
> fr.btlm <- btlm(X = X, Z = Z, XX = XX, tree = c(0.95,
+     2, 10), m0r1 = TRUE)
> fr.btlm.mse <- sqrt(mean((fr.btlm$ZZ.mean - ff$Ytrue)^2))
> fr.btlm.mse
```

Next, fit the GP LLM, and obtain its RMSE.

```
> fr.bgpllm <- bgpllm(X = X, Z = Z, XX = XX, m0r1 = TRUE)
> fr.bgpllm.mse <- sqrt(mean((fr.bgpllm$ZZ.mean - ff$Ytrue)^2))
> fr.bgpllm.mse
```

So, the GP LLM is 3.868 times better than Bayesian linear CART on this data, in terms of RMSE (in terms of MSE the GP LLM is 1.967 times better). Watching the evolution of the Markov chain for the GP LLM (via the progress statements written to `stdout`, not shown because the not would fit on the page), it is easy to see how the GP LLM quickly learns that $\mathbf{b} = (1, 1, 1, 0, 0, 0, 0, 0, 0, 0)$, and that $\beta_4 \approx 4$ and $\beta_5 \approx 10$—basically that only the first three inputs contribute nonlinearly, the fourth and fifth contribute linearly, and the remaining five not at all [10].

3.6 Adaptive Sampling

In this section, sequential design of experiments, a.k.a. *adaptive sampling*, is demonstrated on the exponential data of Section 3.3. Gathering, again, the data:

```
> exp2d.data <- exp2d.rand()
> X <- exp2d.data$X
> Z <- exp2d.data$Z
> Xcand <- exp2d.data$XX
```

Start by fitting a treed GP LLM model to the data, without prediction, in order to infer the MAP tree $\hat{\mathcal{T}}$.

```
> exp1 <- btgpllm(X = X, Z = Z, pred.n = FALSE, corr = "exp")

> tgp.trees(exp1)

NOTICE: skipped plotting tree of height 1, with lpost = 143.976
```

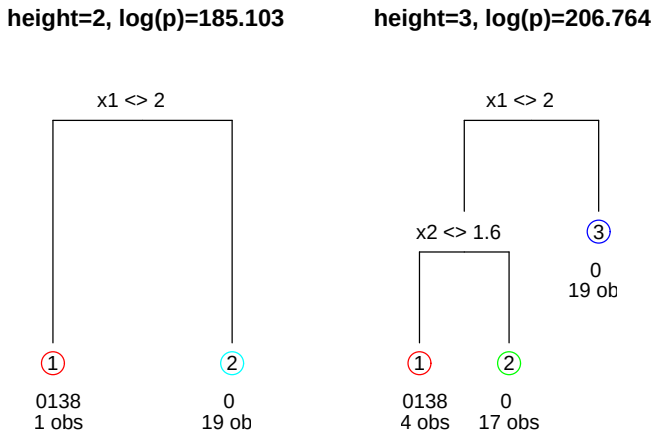

Figure 15: MAP trees of each height encountered in the Markov chain for the exponential data, showing $\hat{\sigma}^2$ and the number of observations n at the leaves. $\hat{\mathcal{T}}$ is the one with the maximum $\log(p)$ above.

The trees are shown in Figure 15. Then, use the `tgp.design` function to create D-optimal candidate designs in each region of $\hat{\mathcal{T}}$.

```
> XX <- tgp.design(10, Xcand, exp1)

sequential treed D-Optimal design in 3 partitions
dopt.gp (1) choosing 2 new inputs from 66 candidates
dopt.gp (2) choosing 3 new inputs from 104 candidates
dopt.gp (3) choosing 6 new inputs from 191 candidates
```

Figure 16 shows the sampled `XX` locations (circles) amongst the input locations `X` (dots) and MAP partition ($\hat{\mathcal{T}}$). Notice how the candidates `XX` are spaced out relative to themselves, and relative to the inputs `X`, unless they are near partition boundaries. The placing of configurations near region boundaries is a symptom particular to D-optimal designs. This is desirable for experiments with `tgp` models, as model uncertainty is usually high there [2].

```
> plot(exp1$X, pch = 19, cex = 0.5)
> points(XX)
> tgp.plot.parts.2d(exp1$parts)
```

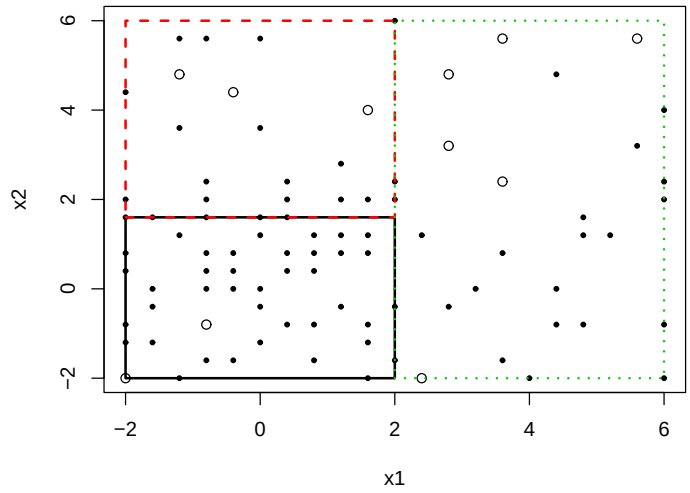

Figure 16: Treed D-optimal candidate locations `XX` (circles), input locations `X` (dots), and MAP tree $\hat{\mathcal{T}}$

Figure 16 uses the `tgp.plot.parts.2d` function. Unfortunately, this function is not well documented in the current version of the `tgp` package. This should change in future versions.

Now, the idea is to fit the treed GP LLM model, again, in order to assess uncertainty in the predictive surface at those new candidate design points. For illustrative purpose, the following code gathers all three adaptive sampling statistics: ALM, ALC, & EGO.

```
> exp1.btgpllm <- btgpllm(X = X, Z = Z, XX = XX, corr = "exp",
+     ego = TRUE, ds2x = TRUE)
```

Figure 17 shows the posterior predictive surface. The error surface, on the *right*, summarizes posterior predictive uncertainty by a norm of quantiles. Since the combined data and predictive locations are not densely packed in the input space, the `loess` smoother may have trouble with the interpolation. One option is increase the `tgp`-default kernel span supplied to `loess`, e.g., `span = 0.5`. Or, the `akima` method can be used instead.

In accordance with the ALM algorithm, candidate locations `XX` with largest predictive error would be sampled (added into the design) next. These are most likely to be in the interesting region, i.e., the first quadrant. However, due to the random nature of this `Sweave` document, this is not always the case. Results

```
> par(mfrow = c(1, 2), bty = "n")
> plot(exp1.btgpllm, main = "treed GP LLM,", method = "akima",
+     layout = "surf")
> plot(exp1.btgpllm, main = "treed GP LLM,", method = "akima",
+     layout = "as", as = "alm")
```

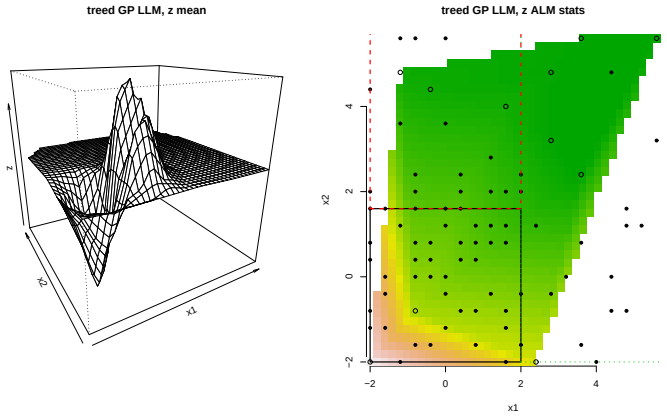

Figure 17: *Left*: Posterior mean surface; *right* ALM adaptive sampling image for (only) candidate locations `XX` (circles), MAP tree $\mathcal{T}$ and input locations `X` (dots). (circles), input locations `X` (dots), and MAP tree $\hat{\mathcal{T}}$

depend heavily on the clumping of the original design in the un-interesting areas, and on the estimate of $\hat{\mathcal{T}}$.

Adaptive sampling via the ALC, or EGO (or both) algorithms proceeds similarly, following the surfaces shown in Figure 18.

A Linking to ATLAS

`ATLAS` [23] is supported as an alternative to standard BLAS and LAPACK for fast, automatically tuned, linear algebra routines. Compared standard `BLAS/Lapack`, those automatically tuned by `ATLAS` are signigantly faster. If you know that `R` has already been linked to tuned linear algebra libraries (e.g., on `OSX`), then compiling with ATLAS as described below, is unncessary—just install as usual. As an alternative to linking `tgp` to ATLAS directly, one could re-compile all of `R` linking it to `ATLAS` following the documentation on the `R` website. While this is arguably best solution since all of `R` benefits, the task can prove challenging to accomplish and may require administrator (root) priviledges. Linking `tgp` with `ATLAS` directly is described here.

Three easy steps (assuming, of course, you have already compiled and installed `ATLAS` – `http://math-atlas.sourceforge.net`) need to be performed before you install the `tgp` package from source.

1. Edit src/Makevars. Comment out the existing `PKG_LIBS` line, and replace

```
> par(mfrow = c(1, 2), bty = "n")
> plot(exp1.btgpllm, main = "treed GP LLM,", method = "akima",
+     layout = "as", as = "alc")
> plot(exp1.btgpllm, main = "treed GP LLM,", method = "akima",
+     layout = "as", as = "ego")
```

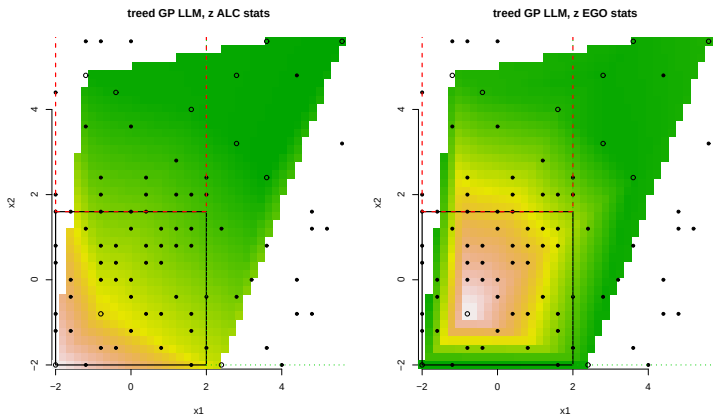

Figure 18: Adaptive sampling images for (only) candidate locations `XX` (circles), MAP tree $\mathcal{T}$ and input locations `X` (dots). (circles), input locations `X` (dots), and MAP tree $\hat{\mathcal{T}}$. *Left*: ALC; *right*: EGO.

it with:

```
PKG_LIBS = -L/path/to/ATLAS/lib -llapack -lcblas -latlas
```

You may need replace `"-llapack -lcblas -latlas"` with whatever ATLAS recommends for your OS. (See `ATLAS` README.) For example, if your ATLAS compilation included F77 support, you might need to add `"-lF77blas"`, if you compiled with pthreads, you would might use `"-llapack -lptcblas -lptf77blas -latlas"`.

2. Continue editing src/Makevars. Add:

```
PKG_CFLAGS = -I/path/to/ATLAS/include
```

3. Edit src/linalg.h and commend out lines 40 & 41:

```
/*#define FORTPACK
#define FORTBLAS*/
```

Now simply install the `tgp` package as usual. Reverse the above instructions to disable ATLAS. Don't forget to re-install the package when you're done.

B Implementation

The treed GP model is coded in a mixture of `C` and `C++`: `C++` for the tree data structure ($\mathcal{T}$) and `C` for the GP at each leaf of $\mathcal{T}$. The code has been tested on Unix (`Solaris, Linux, FreeBSD, OSX`) and Windows (2000, XP) platforms.

It is useful to first translate and re-scale the input data ($\mathbf{X}$) so that it lies in an $\Re^{m_X}$ dimensional unit cube. This makes it easier to construct prior distributions for the width parameters to the correlation function $K(\cdot,\cdot)$. Proposals for all parameters which require MH sampling are taken from a uniform "sliding window" centered around the location of the last accepted setting. For example, a proposed a new nugget parameter g_ν to the correlation function $K(\cdot,\cdot)$ in region r_ν would go as

$$g_\nu^* \sim \text{Unif}\left(\frac{3}{4}g_\nu, \frac{4}{3}g_\nu\right).$$

Calculating the corresponding forward and backwards proposal probabilities for the MH acceptance ratio is straightforward.

After conditioning on the tree and parameters ($\{\mathcal{T}, \boldsymbol{\theta}\}$), prediction can be parallelized by using a producer/consumer model. This allows the use of the `PThreads` libraries in order to take advantage of multiple processors, and get speed-ups of at least a factor of two. The current `tgp` package contains a parallelized implementation, but it is not enabled by default. Documentation explaining how to unleash this feature will be included in future versions. Parallel sampling of the posterior of $\boldsymbol{\theta}|\mathcal{T}$ for each of the $\{\theta_\nu\}_{\nu=1}^R$ is also possible. However, the speed-up in this second case is less impressive, and so is not supported by the current version of the `tgp` package.

References

[1] L. Breiman, J. H. Friedman, R. Olshen, and C. Stone. *Classification and Regression Trees*. Wadsworth, Belmont, CA, 1984.

[2] K. Chaloner and I. Verdinelli. Bayesian experimental design, a review. *Statistical Science*, 10 No. 3:273–1304, 1995.

[3] H. A. Chipman, E. I. George, and R. E. McCulloch. Bayesian CART model search (with discussion). *Journal of the American Statistical Association*, 93:935–960, 1998.

[4] H. A. Chipman, E. I. George, and R. E. McCulloch. Bayesian treed models. *Machine Learning*, 48:303–324, 2002.

[5] D. A. Cohn. Neural network exploration using optimal experimental design. In Jack D. Cowan, Gerald Tesauro, and Joshua Alspector, editors, *Advances in Neural Information Processing Systems*, volume 6(9), pages 679–686. Morgan Kaufmann Publishers, 1996.

[6] N.A. Cressie. *Statistics for Spatial Data*. John Wiley and Sons, Inc., 1991.

[7] Dipak Dey, Peter Müeller, and Debajyoti Sinha. *Practical nonparametric and semiparametric Bayesian statistics*. Springer-Verlag New York, Inc., New York, NY, USA, 1998.

[8] Fields Development Team. fields: Tools for spatial data. National Center for Atmospheric Research, Boulder CO, 2004. URL: http://www.cgd.ucar.edu/Software/Fields.

[9] J. H. Friedman. Multivariate adaptive regression splines. *Annals of Statistics*, 19, No. 1:1–67, March 1991.

[10] R. B. Gramacy. *Bayesian Treed Gaussian Process Models*. PhD thesis, University of California, Santa Cruz, CA 95060, December 2005. Department of Applied Math & Statistics.

[11] R. B. Gramacy, Herbert K. H. Lee, and William Macready. Parameter space exploration with Gaussian process trees. In *ICML*, pages 353–360. Omnipress & ACM Digital Library, 2004.

[12] Robert B. Gramacy and Herbert K H. Lee. Gaussian processes and limiting linear models. Technical report, Dept. of Applied math & Statistics, University of California, Santa Cruz, 2005.

[13] D. Harrison and D. L. Rubinfeld. Hedonic housing prices and the demand for clean air. *Journal of Environmental Economics and Management*, 5:81–102, 1978.

[14] D.R. Jones, M. Schonlau, and W. J. Welch. Efficient global optimization of expensive black box functions. *Journal of Global Optimization*, 13:455–492, 1998.

[15] D. J. C. MacKay. Information-based objective functions for active data selection. *Neural Computation*, 4(4):589–603, 1992.

[16] G. Matheron. Principles of geostatistics. *Economic Geology*, 58:1246–1266, 1963.

[17] R. Neal. Monte carlo implementation of Gaussian process models for Bayesian regression and classification". Technical Report CRG–TR–97–2, Dept. of Computer Science, University of Toronto., 1997.

[18] R Development Core Team. *R: A language and environment for statistical computing*. R Foundation for Statistical Computing, Vienna, Austria, 2004. ISBN 3-900051-00-3.

[19] C.E. Rasmussen and Z. Ghahramani. Infinite mixtures of Gaussian process experts. In *Advances in Neural Information Processing Systems*, volume 14, pages 881–888. MIT Press, 2002.

[20] T. J. Santner, B. J. Williams, and William I. Notz. *The Design and Analysis of Computer Experiments*. Springer-Verlag, New York, NY, 2003.

[21] S. Seo, M. Wallat, T. Graepel, and K. Obermayer. Gaussian process regression: Active data selection and test point rejection. In *Proceedings of the International Joint Conference on Neural Networks*, volume III, pages 241–246. IEEE, July 2000.

[22] B. W. Silverman. Some aspects of the spline smoothing approach to non-parametric curve fitting. *Journal of the Royal Statistical Society Series B*, 47:1–52, 1985.

[23] R. Clint Whaley and Antoine Petitet. `ATLAS` (Automatically Tuned Linear Algebra Software). http://math-atlas.sourceforge.net/, 2004.